Experimental Recent Vector Boson Results

ATLAS & CMS

SM@LHC'25, Durham

Tobias Fitschen[†] *for the ATLAS & CMS Collaborations*

Apr 07 2025

[†]University of Manchester

European Research Council
Established by the European Commission

Why Study Vector Bosons?

SM vector bosons interactions:

$$\mathcal{L}_{\text{Proca}} = -\frac{1}{2} F_{\mu\nu} F^{\nu\mu} + m B_\nu B^\nu$$

Eq of motion: $\partial_\mu F^{\mu\nu} + m^2 B^\nu = 0$

Solved by plane-wave Ansatz: $B^\mu(x) = C \epsilon^\mu(p) e^{-ipx}$

with polarization ϵ^μ

Longitudinal polarisation component ϵ_L proportional to energy:

cartesian		circular+longitudinal
$\epsilon_x = (0; 1, 0, 0)$		$\epsilon_+ = (0; 1, i, 0)$
$\epsilon_y = (0; 0, 1, 0)$	$\rightarrow$	$\epsilon_- = (0; 1, -i, 0)$
$\epsilon_z = (0; 0, 0, 1)$		$\epsilon_L = \frac{1}{m}(p_z; 0, 0, E)$

$\Rightarrow$ Amplitude diverges with $\sqrt{s} = E \rightarrow \infty$

$$\mathcal{A}(V_L V_L \rightarrow V_L V_L)_{\text{s-channel}} \propto -s\ g_W^2$$

This breaks unitarity!

Restoring Unitarity

Example: Scattering of longitudinal W components:

$$\mathcal{A}(W_L W_L \to W_L W_L) \propto g_W^2 \left(-s - t + \frac{s^2}{s - m_H^2} + \frac{t^2}{t - m_H^2} \right)$$

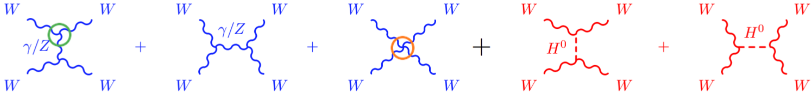

- Divergence from Higgs-less processes cancelled by those with Higgs
- Even small deviations from SM values of quartic and triple gauge couplings would spoil this cancellation:

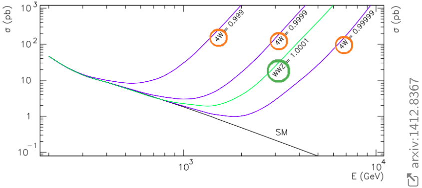

⇒ **Vector boson couplings are highly sensitive probes for SM & BSM**

Toolset: Effective Field Theory (EFT)

Standard Model Effective Field Theory (SMEFT)

Based on Taylor expansion in local operators with mass dimension > 4

With energy scale Λ as effective expansion parameter

$$\mathcal{L}_{\text{EFT}} = \mathcal{L}_{\text{SM}} + \sum_i \frac{c_i}{\Lambda^2}\mathcal{O}_i^{\text{dim-6}} + \sum_j \frac{c_j}{\Lambda^4}\mathcal{O}_j^{\text{dim-8}}$$

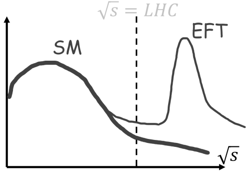

c_i : Dimensionless Wilson coefficients

$\mathcal{O}_i$: EFT operators invariant under SM, suppressed by powers of Λ

- **Dim-6 operators**: Anomalous Triple Gauge Couplings (aTGC): **triboson**
  - $\rightarrow$ Warsaw basis: 2499 operators, reduced to 59 by $U(3)^5$ symmetry
- **Dim-8 operators**: Anomalous Quartic Gauge Couplings (aQGC): **VBS**
  - $\rightarrow$ Eboli basis: 21 operators for aQGC
    - 3 groups: scalar (**S**), transverse (**T**), and mixed (**M**)
  - **Neutral** Anomalous Triple Gauge Couplings (nTGC): **e.g.:** $Z \rightarrow \gamma\gamma$ (nTGC are forbidden at tree level in SM)

(all odd dimensions ops. violate either baryon- or lepton-number conservation)

Toolset: Effective Field Theory (EFT)

Additional terms: Expansion assumes that interference term dominates (lowest Λ power):

$$\textbf{dim-6:}\quad |A_{\text{full}}^{dim-6}|^2 = |A_{\text{SM}}|^2 + \sum_i \frac{c_i}{\Lambda^2} A_{\text{SM}}^\dagger A_i + \sum_i \frac{|c_i|^2}{\Lambda^4}|A_i|^2 + \sum_{i,j,i\neq j} \frac{c_i c_j}{\Lambda^4} A_i^\dagger A_j$$

$$\textbf{dim-8:}\quad |A_{\text{full}}^{dim-8}|^2 = |A_{\text{SM}}|^2 + \sum_i \frac{c_i}{\Lambda^4} A_{\text{SM}}^\dagger A_i + \sum_i \frac{|c_i|^2}{\Lambda^8}|A_i|^2 + \sum_{i,j,i\neq j} \frac{c_i c_j}{\Lambda^8} A_i^\dagger A_j$$

Not necessarily given in all kinematic regions.

$\rightarrow$ Also consider pure EFT term, or even EFT cross-term in signal EFT MC

Clipping: The EFT expansion in Λ is not valid for energies above Λ

$\rightarrow$ "Clip" $\sqrt{\hat{s}} > \Lambda$ and calculate upper limits as function of Λ

- Scan over every cut-off value $\sqrt{\hat{s}}$ depending on the Wilson coefficient (often $\sqrt{\hat{s}} = M_{VV(V)}$)
- Remove all EFT MC events above $\sqrt{\hat{s}}$
- Limits physically meaningful up to intersection with resulting unitarity bound

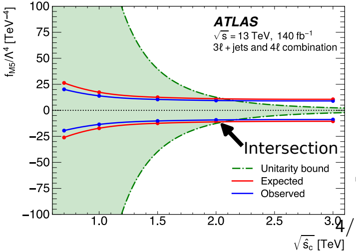

arxiv:2412.15123

New experimental results:

ATLAS Charged-Current DY at High M_T

ATLAS VVZ

ATLAS $Z\gamma$ nTGC

ATLAS Semileptonic VBS ($VVjj$)

CMS Semileptonic VBS ($ZVjj$)

CMS $WZ\gamma$

Charged-Current DY at High M_T

Measurement of double-differential charged-current Drell-Yan cross-sections at high transverse masses in pp collisions at $\sqrt{s} = 13$ TeV with the ATLAS detector

arxiv:2502.21088

EFT constraints:
4 dim-6 fermionic operators

ATLAS EXPERIMENT

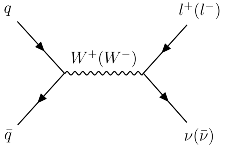

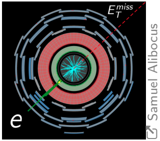

- **First measurement** of $pp \to W^\pm \to \ell^\pm (= e/\mu)\nu$ above resonance region: $m_\mathrm{T}^W > 0.2$ TeV
- Full Run 2 (13 TeV, 140 fb^{-1})
- Single (m_T^W) differential cross-sections up to $m_\mathrm{T}^W < 5$ TeV
  - Double (m_T^W, $|\eta_\ell|$) differential up to $m_\mathrm{T}^W < 2$ TeV
- Unfolded to fiducial SR:

  $|\eta| < 2.4$, $p_\mathrm{T}^\ell > 65$, $p_\mathrm{T}^\nu > 85$ GeV
- Multijet CR: no m_T^W, invert $E_\mathrm{T}^\mathrm{miss}$ cut $\to$ Data driven (matrix method)
- Top CR: require 2 ℓ (dilep $t\bar{t}$)

e^+ signal region

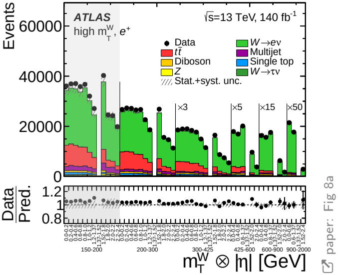

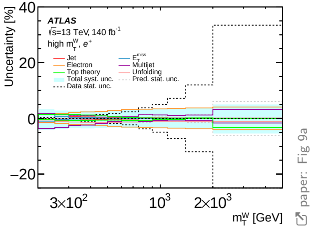

3% precision < 0.8 TeV, statistics dominated beyond

Charged-Current DY at High M_T

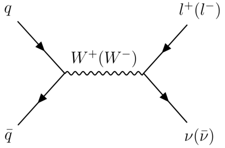

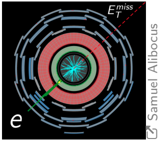

- **First measurement** of $pp \to W^{\pm} \to \ell^{\pm}(= e/\mu)\nu$ above resonance region: $m_T^W > 0.2$ TeV
- Full Run 2 (13 TeV, 140 fb^{-1})
- Single (m_T^W) differential cross-sections up to $m_T^W < 5$ TeV
  - Double (m_T^W, $|\eta_\ell|$) differential up to $m_T^W < 2$ TeV
- Unfolded to fiducial SR:

  $|\eta| < 2.4,\ p_T^\ell > 65,\ p_T^\nu > 85$ GeV
- Multijet CR: no m_T^W, invert E_T^{miss} cut $\to$ Data driven (matrix method)
- Top CR: require 2 ℓ (dilep $t\bar{t}$)

μ^+ signal region

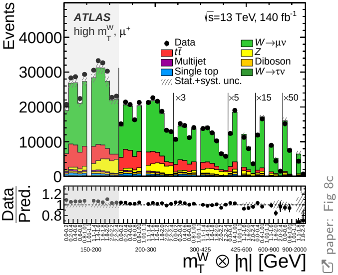

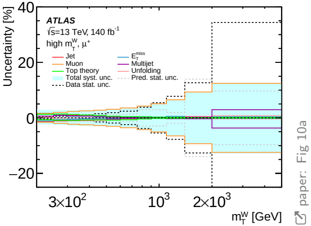

3% precision < 0.8 TeV, statistics dominated beyond

ATLAS EXPERIMENT

Differential cross-section

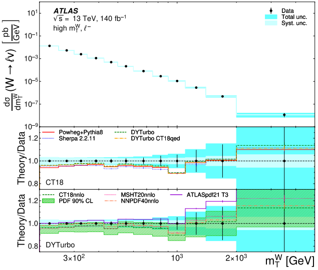

paper: Fig 17a

$\ell^{\pm}$ charge asymmetry $A_\ell = \frac{d\sigma_+ - d\sigma_-}{d\sigma_+ + d\sigma_-}$

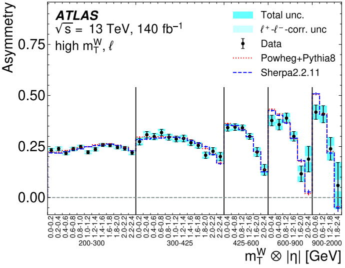

paper: Fig 16b

- Measurements based on single (m_T) and double (m_T, $|\eta_\ell|$) differential cross-sections
- Separate/combined for 4 SRs: e^+, e^-, μ^+, μ^-
- No significant deviation from SM
- NNLO perturbative QCD, NLO EWK effects → constrain PDFs

e/μ lepton-universality

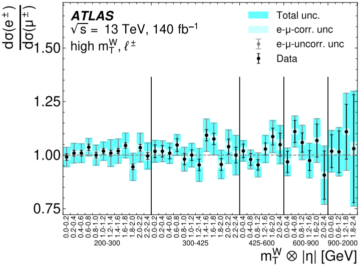

paper: Fig 13b

Charged-Current DY at High M_T

ATLAS EXPERIMENT

EFT Interpretation

- LO predictions modified to account for higher-order QCD & EW corrections:
- Warsaw basis with $U(3)^5$
- SM-EFT interference and pure EFT terms considered in MC
  - Constraints driven by interference terms
- Limits are driven by PDF uncertainty
  - Improve by factor 1.4 - 2.6 when only considering experimental uncertainties

Constraints on 4 dim-6 SMEFT fermion operators:

Wilson Coefficient	Operator
$c_{lq}^{(3)}$	$O_{lq}^{(3)} = (\bar{l}\tau^I\gamma_\mu l)(\bar{q}\tau^I\gamma^\mu q)$
$c_{ll}^{(1)}$	$O_{ll}^{(1)} = (\bar{l}\gamma_\mu l)(\bar{l}\gamma^\mu l)$
$c_{Hl}^{(3)}$	$O_{Hl}^{(3)} = (H^\dagger i \overleftrightarrow{D}_\mu^I H)(\bar{l}\tau^I\gamma^\mu l)$
$c_{Hq}^{(3)}$	$O_{Hq}^{(3)} = (H^\dagger i \overleftrightarrow{D}_\mu^I H)(\bar{q}\tau^I\gamma^\mu q)$

paper: Tab 2

Observed limits

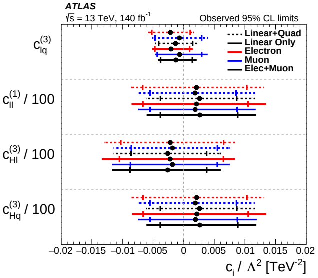

paper: Fig 21b

- Quark-lepton contact operator $\mathcal{O}_{lq}^{(3)}$: significance enhancement at high m_T^W
- Other 3 operators: constant scaling without m_T^W dependence

VVZ

Observation of VVZ production at $\sqrt{s} = 13$ TeV with the ATLAS detector

arxiv:2412.15123

EFT constraints:
4 dim-8 mixed (M) aQGC operators

VVZ

- Full Run 2 (13 TeV, 140 fb^{-1})
- Occurs in only 1 in 10^{-12} pp interactions
- 7 decay channels with highest significance

  $\rightarrow$ 12 analysis regions (7 SR + 5 CR)

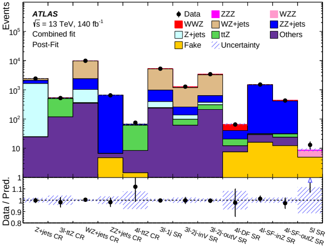

paper: Fig 2

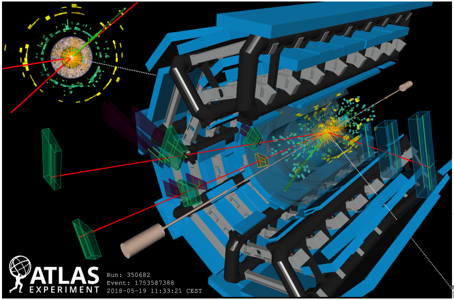

home.cern/news

$VVZ = (W \rightarrow e\nu)(W \rightarrow \mu\nu)(Z \rightarrow \mu\mu)$

candidate event

mono-V vertices

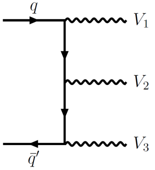

triple-V coupling

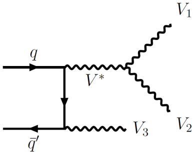

quartic-V coupling

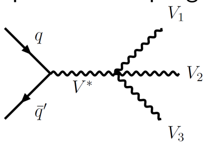

Higgsstrahlung

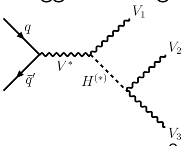

paper: Fig 1

- First observation of VVZ (6.4 σ),
- Evidence for WWZ (4.4 σ)
- Search for WZZ (2.8 σ)
- No ZZZ region due to low cross-section
- Signal strengths compatible with SM
- Previously observed:
  - WWW (8.0 σ ATLAS, 2022)
  - VVV (5.7 σ CMS, 2020)
- Previous evidence:
  - WWZ (3.4 σ CMS, 2020)

Individual BDT in each SR

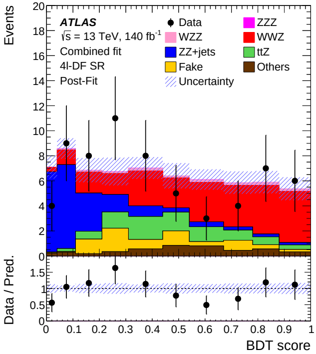

paper: Fig 3d

Process	Signal strength	Cross section (fb)	Observed (expected) sensitivity
VVZ	$1.43 \pm 0.20(\text{stat.})^{+0.21}_{-0.19}(\text{syst.})$	$660^{+93}_{-90}(\text{stat.})^{+88}_{-81}(\text{syst.})$	6.4 (4.7) σ
WWZ	$1.33 \pm 0.28(\text{stat.})^{+0.21}_{-0.17}(\text{syst.})$	$442 \pm 94(\text{stat.})^{+60}_{-52}(\text{syst.})$	4.4 (3.6) σ
WZZ	$2.13^{+1.18}_{-0.96}(\text{stat.})^{+0.76}_{-0.41}(\text{syst.})$	$200^{+111}_{-91}(\text{stat.})^{+65}_{-37}(\text{syst.})$	2.8 (1.6) σ

paper: Tab 6

ATLAS EXPERIMENT

- Limits on aQGC via 4 dim-8 EFT coefficients (Eboli basis)
- From simultaneous fit to 3ℓ & 4ℓ channels
- BDT trained on EFT signal in each SR
- Limits unitarized with clipping parameter $\sqrt{\hat{s}_c}$

Clipping scan for Wilson coefficient f_{M5}

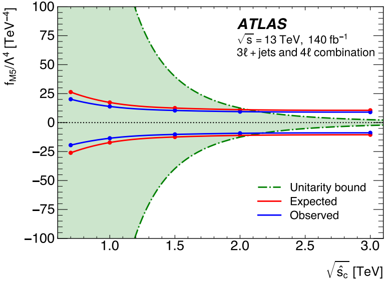

paper: Fig 5d

- $\sqrt{\hat{s}_c} = m_{\max}(V_i,\ V_j)$: maximum of the three diboson invariant mass combinations

Unitarized limits

Coefficient	Expected limit [TeV^{-4}]	Exp. $\sqrt{\hat{s}_c}$ [TeV]	Observed limit [TeV^{-4}]	Obs. $\sqrt{\hat{s}_c}$ [TeV]
f_{M2}/Λ^4	[−18, 17]	1.2	[−19, 19]	1.2
f_{M3}/Λ^4	[−28, 29]	1.5	[−28, 29]	1.5
f_{M4}/Λ^4	[−14, 14]	1.6	[−12, 12]	1.7
f_{M5}/Λ^4	[−11, 11]	2.1	[−9.1, 9.3]	2.2

paper: Tab 8

Limits consistent with those from $W\gamma jj$ (ATLAS, CMS)

$Z\gamma$ nTGC

Measurements of $Z\gamma$ differential cross sections and search for neutral triple gauge couplings in pp collisions at $\sqrt{s} = 13$ TeV with the ATLAS detector

ATLAS-CONF-2025-001

EFT constraints:
4 dim-8 nTGC coefficients and form factors

- Improvements on 2023 paper
- Dedicated region to enhance nTGC
  - High $p_T^\gamma > 200$ GeV
  - Jet veto & narrow m_Z window
- Previous: Conventional form factors
  - Only satisfies $U(1)$ (unphysical)
- New: nTGC form factors
  - Satisfy full $SU(2)_L \times U(1)$
- Up to 2 orders of magnitude difference
- More in Elvira's presentation

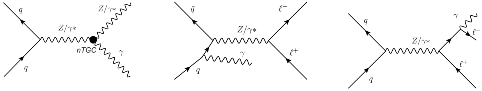

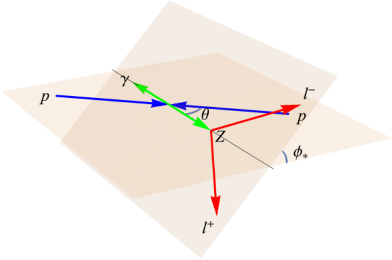

Wilson coefficients

Parameters	Current limits at 95% C.L. (140 fb^{-1}) using new formalism		Limits at 95% C.L. from Reference [59] (36.1 fb^{-1}) using old formalism	
	Observed 95% C.L. [TeV^{-4}]	Expected 95% C.L. [TeV^{-4}]	Observed 95% C.L. [TeV^{-4}]	Expected 95% C.L. [TeV^{-4}]
C_{BB}/Λ^4	[-0.37, 0.37]	[-0.44, 0.44]	[-0.24, 0.24]	[-0.28, 0.27]
$C_{\tilde{B}W}/\Lambda^4$	[-0.54, 0.53]	[-0.62, 0.61]	[-1.1, 1.1]	[-1.3, 1.3]
C_{BW}/Λ^4	[-0.87, 0.95]	[-1.05, 1.14]	[-0.65, 0.64]	[-0.74, 0.74]
C_{WW}/Λ^4	[-1.90, 1.78]	[-2.26, 2.13]	[-2.3, 2.3]	[-2.7, 2.7]

paper: Tab 8

ATLAS EXPERIMENT

- Improvements on 2023 paper
- Dedicated region to enhance nTGC
    - High $p_T^{\gamma} > 200$ GeV
    - Jet veto & narrow m_Z window
- Previous: Conventional form factors
    - Only satisfies $U(1)$ (unphysical)
- New: nTGC form factors
    - Satisfy full $SU(2)_L \times U(1)$
- Up to 2 orders of magnitude difference
- More in Elvira's presentation

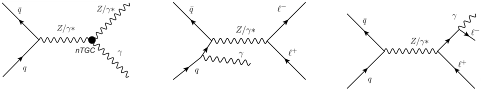

paper: Fig 1

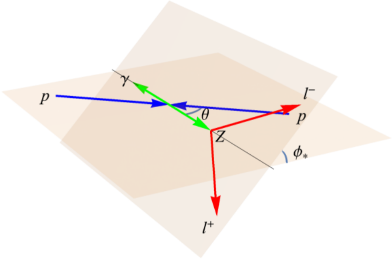

paper: Fig 2

Form factors

Parameters	Current limits at 95% C.L. (140 fb^{-1}) using new formalism		Limits at 95% C.L. from Reference [59] (36.1 fb^{-1}) using old formalism	
	Observed 95% C.L.	Expected 95 % C.L.	Observed 95% C.L.	Expected 95 % C.L.
h_4^{γ}	$[-1.3\times10^{-5}, 1.4\times10^{-5}]$	$[-1.5\times10^{-5}, 1.6\times10^{-5}]$	$[-4.4\times10^{-7}, 4.3\times10^{-7}]$	$[-5.1\times10^{-7}, 5.0\times10^{-7}]$
h_4^{Z}	$[-2.4\times10^{-5}, 2.6\times10^{-5}]$	$[-2.8\times10^{-5}, 3.0\times10^{-5}]$	$[-4.5\times10^{-7}, 4.4\times10^{-7}]$	$[-5.3\times10^{-7}, 5.1\times10^{-7}]$
h_3^{γ}	$[-3.5\times10^{-4}, 4.6\times10^{-4}]$	$[-4.0\times10^{-4}, 4.9\times10^{-4}]$	$[-3.7\times10^{-4}, 3.7\times10^{-4}]$	$[-4.2\times10^{-4}, 4.3\times10^{-4}]$
h_3^{Z}	$[-3.2\times10^{-4}, 3.2\times10^{-4}]$	$[-3.7\times10^{-4}, 3.6\times10^{-4}]$	$[-3.2\times10^{-4}, 3.3\times10^{-4}]$	$[-3.8\times10^{-4}, 3.8\times10^{-4}]$

paper: Tab 9

ATLAS EXPERIMENT

Semileptonic VBS ($VVjj$)

Electroweak diboson production in association with a high-mass dijet system in semileptonic final states from pp collisions at $\sqrt{s} = 13$ TeV with the ATLAS detector

arxiv:2503.17461

EFT constraints:
18 dim-8 aQGC operators in Eboli basis

Semileptonic VBS ($VVjj$)

- EWK VVjj measurement
- Full Run 2 (13 TeV, 140 fb^{-1})
- Semi-lep channel: high aQGC sensitivity

Experimental Signature:

- 2 forward, back-to-back jets $(jj)^{\text{tag}}$
- One boson decays hadronically:

  2 $R = 0.4$ signal jets (resolved)
  or 1 $R = 1.0$ signal jet (merged)

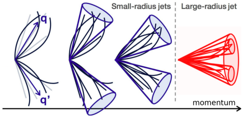

resolved merged

- One boson decays leptonically:
  - 0-lepton: $Z \to \nu\nu$, $W \to \nu\not{\ell}$
  - 1-lepton: $W \to \ell\nu$, $Z \to \ell\not{\ell}$
  - 2-lepton: $Z \to \ell\ell$

Simultaneous fit in 9 SRs + 9 CRs

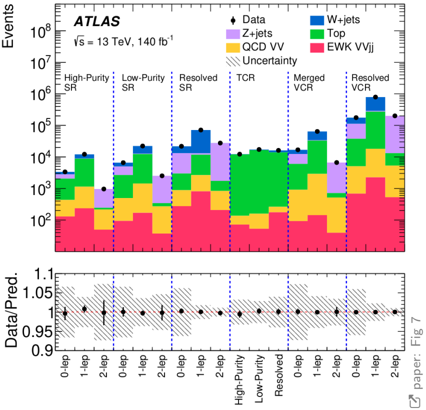

paper: Fig 7

VBS EWK $VVjj$

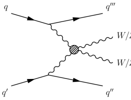

relevant for aQGC EFT

non-VBS EWK $VVjj$

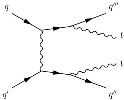

non-VBS QCD $VVjj$

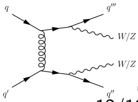

paper: Fig 1

Semileptonic VBS ($VVjj$)

Final discriminant:

- Recurrent NN (RNN) on up to 5 jets (p_T, η, ϕ, E, n_{tracks}) + large-R jet in merged regime

Results

- First observation of EWK VVjj in semileptonic decay (7.4 σ)
- In fiducial VBS phase space
- EWK and QCD associated VVjj production measured in 2D fit
- Individual limits on 0,1,3-ℓ channels & merged, resolved decay
- No significant deviation from SM

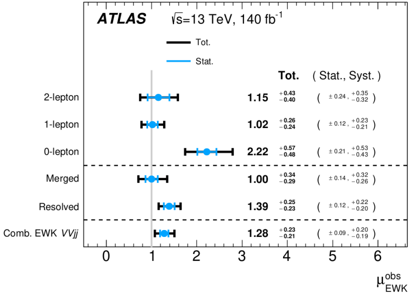

paper: Fig 9

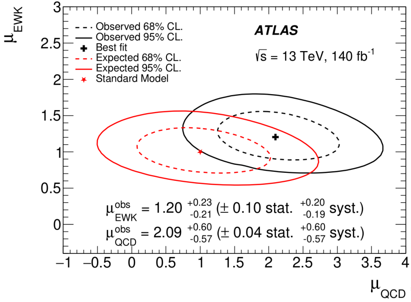

paper: Fig 10

Semileptonic VBS (*VVjj*)

ATLAS EXPERIMENT

- Limits to 18 dim-8 aQGC coefficients in Eboli basis
- Each SR is further split into low/high M_{VV} region to increase sensitivity
  - 1,2-lep: at 1.5 TeV
  - 0-lep: at 1.05 (merged), 1.2 (resolved) TeV

Wilson coefficient	Expected limit [TeV^{-4}]	Observed limit [TeV^{-4}]	Expected limit unitarized [TeV^{-4}]	Observed limit unitarized [TeV^{-4}]
f_{T0}/Λ^4	[-0.20, 0.18]	[-0.25, 0.22]	[-0.79, 0.47] at [1.76, 1.96] TeV	[-0.85, 0.47] at [1.73, 2.00] TeV
f_{T1}/Λ^4	[-0.19, 0.19]	[-0.24, 0.24]	[-0.34, 0.34] at [2.59, 2.59] TeV	[-0.43, 0.43] at [2.43, 2.43] TeV
f_{T2}/Λ^4	[-0.44, 0.44]	[-0.55, 0.55]	[-0.95, 0.96] at [2.22, 2.22] TeV	[-1.16, 1.17] at [2.12, 2.11] TeV
f_{T3}/Λ^4	[-0.38, 0.38]	[-0.48, 0.48]	[-0.62, 0.62] at [2.71, 2.71] TeV	[-0.88, 0.88] at [2.49, 2.48] TeV
f_{T4}/Λ^4	[-1.46, 1.32]	[-1.51, 1.37]	[-3.03, 2.60] at [2.02, 2.09] TeV	[-3.03, 2.60] at [2.02, 2.10] TeV
f_{T5}/Λ^4	[-0.57, 0.53]	[-0.64, 0.58]	-	[-2.65, 2.57] at [1.53, 1.54] TeV
f_{T6}/Λ^4	[-0.76, 0.72]	[-0.74, 0.71]	[-2.82, 2.01] at [1.66, 1.73] TeV	[-2.98, 2.62] at [1.64, 1.69] TeV
f_{T7}/Λ^4	[-1.78, 1.52]	[-1.94, 1.70]	[-7.88, 4.29] at [1.65, 1.90] TeV	[-6.70, 4.11] at [1.72, 1.91] TeV
f_{T8}/Λ^4	[-0.59, 0.59]	[-0.48, 0.48]	-	-
f_{T9}/Λ^4	[-1.22, 1.22]	[-1.02, 1.03]	-	-
f_{S02}/Λ^4	[-3.22, 3.22]	[-3.96, 3.96]	[-5.53, 5.54] at [2.07, 2.67] TeV	[-6.16, 6.17] at [2.01, 2.01] TeV
f_{S1}/Λ^4	[-6.84, 6.86]	[-8.06, 8.06]	-	-
f_{M0}/Λ^4	[-1.13, 1.12]	[-1.26, 1.25]	[-2.61, 2.58] at [2.00, 2.00] TeV	[-2.71, 2.65] at [1.97, 1.98] TeV
f_{M1}/Λ^4	[-3.23, 3.24]	[-3.95, 3.95]	[-6.22, 6.22] at [2.27, 2.27] TeV	[-7.42, 7.43] at [2.17, 2.17] TeV
f_{M2}/Λ^4	[-1.66, 1.67]	[-1.85, 1.85]	-	-
f_{M3}/Λ^4	[-5.29, 5.29]	[-5.68, 5.71]	[-23.69, 23.39] at [1.57, 1.57] TeV	[-18.62, 19.10] at [1.66, 1.65] TeV
f_{M4}/Λ^4	[-2.62, 2.62]	[-2.96, 2.97]	-	-
f_{M5}/Λ^4	[-3.81, 3.82]	[-4.41, 4.44]	[-6.80, 6.80] at [2.33, 2.33] TeV	[-7.28, 7.30] at [2.29, 2.29] TeV
f_{M7}/Λ^4	[-5.32, 5.20]	[-6.60, 6.43]	[-9.47, 9.38] at [2.43, 2.43] TeV	[-11.91, 11.11] at [2.29, 2.33] TeV

paper: Tab 5

$\mathcal{O}_{S0}$ & $\mathcal{O}_{S2}$ are hermitian conjugates, hence: varied simultaneously as $\mathcal{O}_{S02}$

- Clipping with respect to m_{VV} to avoid unitarity violations
- Improves on previous ATLAS searches in all M & S operators
  - T operators still best constrained by $Z(\rightarrow \nu\bar{\nu})\gamma jj$ analysis

$$|A_{\text{full}}^{dim-8}|^2 = |A_{\text{SM}}|^2 + \sum_i \frac{f_i}{\Lambda^4} A_{\text{SM}}^\dagger A_i + 2\sum_i \frac{|f_i|^2}{\Lambda^8}|A_i|^2 + \sum_{i,j,i\neq j} \frac{f_i f_j}{\Lambda^8} A_i^\dagger A_j$$

- Individual MC samples for SM-EFT interference and pure EFT

- Limits to 18 dim-8 aQGC coefficients in Eboli basis
- Each SR is further split into low/high M_{VV} region to increase sensitivity
  - 1,2-lep: at 1.5 TeV
  - 0-lep: at 1.05 (merged), 1.2 (resolved) TeV

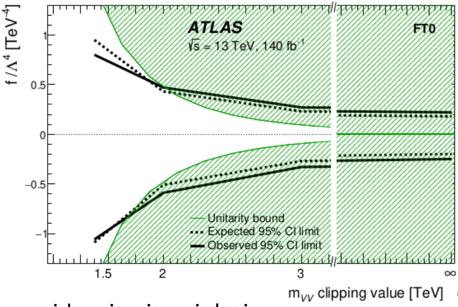

paper: Fig 12a

- Clipping with respect to m_{VV} to avoid unitarity violations
- Improves on previous ATLAS searches in all M & S operators
  - T operators still best constrained by $Z(\rightarrow \nu\bar{\nu})\gamma jj$ analysis

$$|A^{dim-8}_{\text{full}}|^2 = |A_{\text{SM}}|^2 + \sum_i \frac{f_i}{\Lambda^4} A^{\dagger}_{\text{SM}} A_i + 2\sum_i \frac{|f_i|^2}{\Lambda^8}|A_i|^2 + \sum_{i,j,i\neq j} \frac{f_i f_j}{\Lambda^8} A^{\dagger}_i A_j$$

- Individual MC samples for SM-EFT interference and pure EFT

Semileptonic VBS ($ZVjj$)

Study of vector boson scattering in the semileptonic final state and search for anomalous quartic gauge couplings from proton-proton collisions at $\sqrt{s} = 13$ TeV

CMS-PAS-SMP-22-011

EFT constraints:
20 dim-8 aQGC coefficients in Eboli basis

Semileptonic VBS (*ZVjj*)

- Full Run 2 (13 TeV, 138 fb^{-1})
- Mearured EWK *ZVjj* cross-section (1.3 σ, $\mu = 0.63^{+0.53}_{-0.51}$)

Experimental signature

- 2 forward, back-to-back jets
- 2 isolated $\ell = \mu, e$ from Z
- Hadronically decaying V:

  2 AK4 signal jets (resolved)

  or 1 AK8 signal jet (merged)
- SR split into $b-$tag/veto

  (DeepCSV tagger)

Final Discriminant: DNN

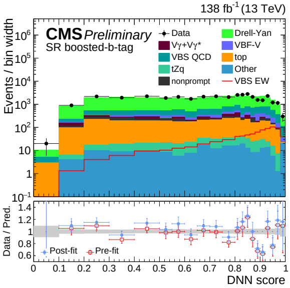

paper: Fig 3a

EWK VBS process

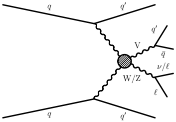

paper: Fig 1

Preselection	$n_{\text{leptons}} = 2$, $m_{\ell\ell} \in [76, 106]$ GeV, $p_T(\ell_1) > 35$ GeV, $p_T(\ell_2) > 20$ GeV, $p_T(j_{1,2}) > 30$ GeV, $m_{jj} > 500$ GeV, $\Delta\eta_{jj} > 2.5$		
Regions	Variables	Lepton Selection	Other Requirements
Signal Region (SR)	65 GeV $< m_V <$ 105 GeV	Same Flavor	Split in b-tag and b-veto
DY Control Region (DY CR)	$m_V <$ 65 GeV, $m_V >$ 105 GeV	Same Flavor	Split in b-tag and b-veto
Top Control Region (Top CR)	65 GeV $< m_V <$105 GeV	Opposite Flavor	-

paper: Tab 1

Semileptonic VBS ($ZVjj$)

- Limits to 20 dim-8 aQGC coefficients in Eboli basis
- Separate for WZ, ZV, combined

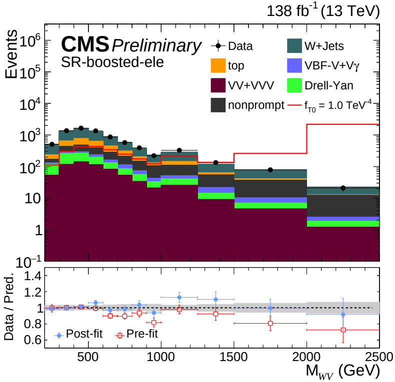

paper: Fig 5a

	Observed (WV) (TeV^{-4})	Expected (WV) (TeV^{-4})	Observed (ZV) (TeV^{-4})	Expected (ZV) (TeV^{-4})	Observed (TeV^{-4})	Expected (TeV^{-4})
f_{S0}/Λ^4	[-3.01, 3.1]	[-4.7, 4.77]	[-9.76, 9.89]	[-13.9, 14.0]	[-2.86, 2.96]	[-4.68, 4.75]
f_{S1}/Λ^4	[-4.27, 4.32]	[-6.56, 6.6]	[-10.2, 10.3]	[-13.9, 13.9]	[-3.97, 4.02]	[-6.45, 6.49]
f_{S2}/Λ^4	[-4.42, 4.48]	[-6.81, 6.86]	[-9.75, 9.89]	[-13.9, 14.0]	[-4.04, 4.11]	[-6.68, 6.73]
f_{M0}/Λ^4	[-0.568, 0.567]	[-0.844, 0.843]	[-1.38, 1.38]	[-1.74, 1.74]	[-0.539, 0.534]	[-0.828, 0.827]
f_{M1}/Λ^4	[-1.71, 1.75]	[-2.6, 2.63]	[-3.97, 4.00]	[-5.28, 5.29]	[-1.59, 1.62]	[-2.55, 2.58]
f_{M2}/Λ^4	[-0.746, 0.747]	[-1.11, 1.11]	[-1.86, 1.86]	[-2.37, 2.37]	[-0.703, 0.703]	[-1.1, 1.1]
f_{M3}/Λ^4	[-2.81, 2.81]	[-4.2, 4.2]	[-5.60, 5.59]	[-7.47, 7.47]	[-2.55, 2.55]	[-4.08, 4.07]
f_{M4}/Λ^4	[-1.74, 1.73]	[-2.6, 2.59]	[-2.70, 2.70]	[-3.61, 3.61]	[-1.48, 1.48]	[-2.42, 2.41]
f_{M5}/Λ^4	[-2.53, 2.51]	[-3.77, 3.76]	[-3.80, 3.81]	[-5.21, 5.23]	[-2.14, 2.13]	[-3.5, 3.5]
f_{M7}/Λ^4	[-2.86, 2.82]	[-4.35, 4.32]	[-6.09, 6.07]	[-8.26, 8.24]	[-2.63, 2.58]	[-4.24, 4.2]
f_{T0}/Λ^4	[-0.096, 0.083]	[-0.14, 0.128]	[-0.26, 0.25]	[-0.33, 0.32]	[-0.0921, 0.0785]	[-0.138, 0.127]
f_{T1}/Λ^4	[-0.0933, 0.1]	[-0.142, 0.149]	[-0.22, 0.24]	[-0.30, 0.31]	[-0.0863, 0.0943]	[-0.14, 0.147]
f_{T2}/Λ^4	[-0.225, 0.225]	[-0.336, 0.335]	[-0.56, 0.60]	[-0.74, 0.76]	[-0.21, 0.214]	[-0.331, 0.332]
f_{T3}/Λ^4	[-0.206, 0.206]	[-0.311, 0.31]	[-0.48, 0.51]	[-0.64, 0.66]	[-0.191, 0.194]	[-0.305, 0.305]
f_{T4}/Λ^4	[-1.09, 1.02]	[-1.58, 1.53]	[-1.44, 1.37]	[-1.84, 1.77]	[-0.895, 0.828]	[-1.4, 1.35]
f_{T5}/Λ^4	[-0.287, 0.257]	[-0.391, 0.383]	[-0.59, 0.57]	[-0.76, 0.73]	[-0.265, 0.237]	[-0.382, 0.373]
f_{T6}/Λ^4	[-0.656, 0.627]	[-0.976, 0.954]	[-0.73, 0.71]	[-0.94, 0.92]	[-0.5, 0.478]	[-0.794, 0.775]
f_{T7}/Λ^4	[-0.936, 0.899]	[-1.39, 1.36]	[-1.78, 1.67]	[-2.26, 2.16]	[-0.85, 0.8]	[-1.34, 1.29]
f_{T8}/Λ^4	–	–	[-0.53, 0.53]	[-0.67, 0.67]	[-0.53, 0.53]	[-0.67, 0.67]
f_{T9}/Λ^4	–	–	[-1.17, 1.16]	[-1.47, 1.45]	[-1.17, 1.16]	[-1.47, 1.45]

paper: Tab 4

- SM-EFT interference and pure EFT terms considered
- Including systematic uncertainties on EFT signal
  - Was not done in previous CMS result

$WZ\gamma$

Measurement of $WZ\gamma$ production and constraints on new physics scenarios in proton-proton collisions at $\sqrt{s} = 13$ TeV

CMS-PAS-SMP-22-018

EFT constraints:

6 dim-8 transverse (T) aQG operators in Eboli basis

- Full Run 2 (13 TeV, 138 fb^{-1})
- Observed $WZ\gamma$ (5.4 σ)

  $\mu_{\text{SR}}^{\text{obs}} = 1.47 \pm 0.15(\text{syst})$

  $\pm\, 0.11(\text{theo}) \pm 0.25(\text{stat})$
- Limits on axion-like particles
- 3 charged leptons from $WZ \to \ell\nu\ell'\ell'$, $\ell\ell' = e, \mu$ + 1 γ

Signal region

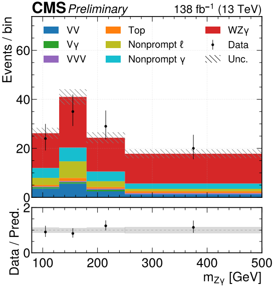

paper: Fig 2d

QGC TGC multipheral ALP$\to Z\gamma$

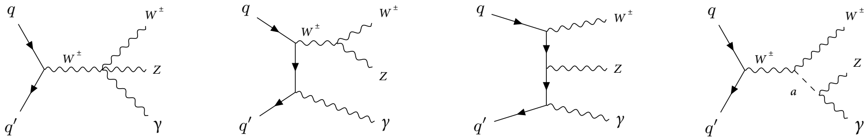

paper: Fig 1

Region	N_ℓ	N_γ	N_{OSSF}	N_{btag}	MET [GeV]	$p_{\text{T}}\{\ell_{Z1},\ell_{Z2},\ell_W,\ell_4\}$ [GeV]	$\min(m(\ell\ell'))$ [GeV]	$\lvert m(\ell_{Z1},\ell_{Z2}) - m_Z\rvert$ [GeV]	$m(\ell_{Z1},\ell_{Z2},\ell_W)$ [GeV]	$m(l_W,\gamma)$ [GeV]
SR	=3	≥ 1	≥ 1	=0	>30	>{25,15,25}	>4	<15	>100	<75 or >105
ZZ CR	=4	—	≥ 1	=0	<30	>{25,15,25,15}	>4	<15	>100	—
Nonprompt ℓ CR	=3	—	≥ 1	>0	>30	>{25,15,25}	>4	>15	>100	—
Nonprompt γ CR	=2	≥ 1	=1	>0	<30	>{25,15}	>4	>15	—	—

paper: Tab 1

- Full Run 2 (13 TeV, 138 fb^{-1})
- Observed $WZ\gamma$ (5.4 σ)

  $\mu_{SR}^{obs} = 1.47 \pm 0.15(\text{syst})$

  $\pm\, 0.11(\text{theo}) \pm 0.25(\text{stat})$
- Limits on axion-like particles
- 3 charged leptons from $WZ \to \ell\nu\ell'\ell'$, $\ell\ell' = e, \mu$ + 1 γ

ALP$\to Z\gamma$ limits

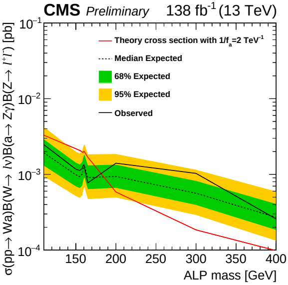

paper: Fig 3a

QGC

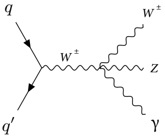

TGC

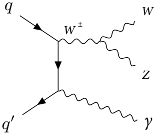

multipheral

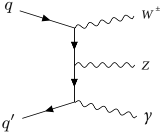

ALP$\to Z\gamma$

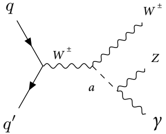

paper: Fig 1

Region	N_ℓ	N_γ	N_{OSSF}	N_{btag}	MET [GeV]	$p_T\{\ell_{Z1},\ell_{Z2},\ell_W,\ell_4\}$ [GeV]	$\min(m(\ell\ell'))$ [GeV]	$\lvert m(\ell_{Z1},\ell_{Z2}) - m_Z\rvert$ [GeV]	$m(\ell_{Z1},\ell_{Z2},\ell_W)$ [GeV]	$m(l_W,\gamma)$ [GeV]
SR	=3	≥ 1	≥ 1	=0	>30	>{25,15,25}	>4	<15	>100	<75 or >105
ZZ CR	=4	—	≥ 1	=0	<30	>{25,15,25,15}	>4	<15	>100	—
Nonprompt ℓ CR	=3	—	≥ 1	>0	>30	>{25,15,25}	>4	>15	>100	—
Nonprompt γ CR	=2	≥ 1	=1	>0	<30	>{25,15}	>4	>15	—	—

paper: Tab 1

- Limits on 6 dim-8 aQGC operators (Eboli basis)
- SM-EFT interference and pure EFT terms considered
- Using invariant mass $m_{\ell\ell\ell\gamma}$
- Quadratic function fit to ratio of aQGC / SM yields in final $m_{\ell\ell\ell\gamma}$ bin
- Unitarity bound determined with VBFNLO framework
- No significant deviation from SM observed

Operators	Observed limits [TeV^{-4}]	Expected limits [TeV^{-4}]	Unitarity bound [TeV]
$F_{T,0}/\Lambda^4$	[-2.60, 2.60]	[-2.52, 2.52]	1.32
$F_{T,1}/\Lambda^4$	[-3.28, 3.24]	[-3.18, 3.14]	1.48
$F_{T,2}/\Lambda^4$	[-7.15, 7.05]	[-6.95, 6.85]	1.35
$F_{T,5}/\Lambda^4$	[-2.54, 2.56]	[-2.46, 2.50]	1.55
$F_{T,6}/\Lambda^4$	[-3.18, 3.22]	[-3.08, 3.14]	1.61
$F_{T,7}/\Lambda^4$	[-6.85, 7.05]	[-6.65, 6.85]	1.71

paper: Tab 4

Summary

EFT constraints by presented analyses:

- ATLAS Charged-Current DY at High M_T: 4 dim-6 fermionic operators
- ATLAS VVZ: 4 dim-8 mixed (M) operators
- ATLAS $Z\gamma$ nTGC: 4 dim-8 nTGC coefficients & form factors
- ATLAS Semileptonic VBS ($VVjj$): 18 dim-8 aQGC operators
- CMS Semileptonic VBS ($ZVjj$): 20 dim-8 aQGC operators
- CMS $WZ\gamma$: 6 dim-8 transverse (T) aQGC operators

Outlook

- Many EFT constraints set with full Run 2 dataset
- Run 3: Promising for EFT with more statistics and higher $\sqrt{s}$

Appendix

aQGC Dimension 8 EFT Operators (Eboli Basis)

Eboli basis

- 21 Operators
- Parametrize anomalous quartic gauge couplings (aQGC)

Experimental handles:

Vector boson scattering (VBS)

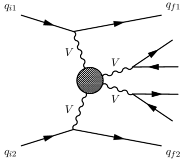

Triboson production

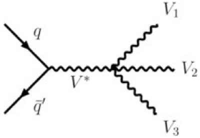

Contributions to vertices of 4 bosons:

	allowed at tree-level SM					not allowed			
	$WWWW$	$WWZZ$	$WW\gamma Z$	$WW\gamma\gamma$	$ZZZZ$	$ZZZ\gamma$	$ZZ\gamma\gamma$	$Z\gamma\gamma\gamma$	$\gamma\gamma\gamma\gamma$
$\mathcal{O}_{S,0}$, $\mathcal{O}_{S,1}$	✓	✓			✓				
$\mathcal{O}_{M,0}$, $\mathcal{O}_{M,1}$, $\mathcal{O}_{M,6}$, $\mathcal{O}_{M,7}$	✓	✓	✓	✓	✓	✓	✓		
$\mathcal{O}_{M,2}$, $\mathcal{O}_{M,3}$, $\mathcal{O}_{M,4}$, $\mathcal{O}_{M,5}$		✓	✓	✓	✓	✓	✓		
$\mathcal{O}_{T,0}$, $\mathcal{O}_{T,1}$, $\mathcal{O}_{T,2}$	✓	✓	✓	✓	✓	✓	✓	✓	✓
$\mathcal{O}_{T,5}$, $\mathcal{O}_{T,6}$, $\mathcal{O}_{T,7}$		✓	✓	✓	✓	✓	✓	✓	✓
$\mathcal{O}_{T,8}$, $\mathcal{O}_{T,9}$					✓	✓	✓	✓	✓

↗ Falke

S (scalar) operators

affect longitudinal polarization

$$\mathcal{O}_{S,0} = \left[(D_\mu\Phi)^\dagger D_\nu\Phi\right] \times \left[(D^\mu\Phi)^\dagger D^\nu\Phi\right]$$
$$\mathcal{O}_{S,1} = \left[(D_\mu\Phi)^\dagger D^\mu\Phi\right] \times \left[(D_\nu\Phi)^\dagger D^\nu\Phi\right]$$
$$\mathcal{O}_{S,2} = \left[(D_\mu\Phi)^\dagger D_\nu\Phi\right] \times \left[(D^\nu\Phi)^\dagger D^\mu\Phi\right]$$

T (transverse) operators

affect transverse polarization

$$\mathcal{O}_{T,0} = \mathrm{Tr}\left[\widehat{W}_{\mu\nu}\widehat{W}^{\mu\nu}\right] \times \mathrm{Tr}\left[\widehat{W}_{\alpha\beta}\widehat{W}^{\alpha\beta}\right] \quad , \quad \mathcal{O}_{T,1} = \mathrm{Tr}\left[\widehat{W}_{\alpha\nu}\widehat{W}^{\mu\beta}\right] \times \mathrm{Tr}\left[\widehat{W}_{\mu\beta}\widehat{W}^{\alpha\nu}\right]$$
$$\mathcal{O}_{T,2} = \mathrm{Tr}\left[\widehat{W}_{\alpha\mu}\widehat{W}^{\mu\beta}\right] \times \mathrm{Tr}\left[\widehat{W}_{\beta\nu}\widehat{W}^{\nu\alpha}\right] \quad , \quad \mathcal{O}_{T,5} = \mathrm{Tr}\left[\widehat{W}_{\mu\nu}\widehat{W}^{\mu\nu}\right] \times B_{\alpha\beta}B^{\alpha\beta}$$
$$\mathcal{O}_{T,6} = \mathrm{Tr}\left[\widehat{W}_{\alpha\nu}\widehat{W}^{\mu\beta}\right] \times B_{\mu\beta}B^{\alpha\nu} \quad , \quad \mathcal{O}_{T,7} = \mathrm{Tr}\left[\widehat{W}_{\alpha\mu}\widehat{W}^{\mu\beta}\right] \times B_{\beta\nu}B^{\nu\alpha}$$
$$\mathcal{O}_{T,8} = B_{\mu\nu}B^{\mu\nu}B_{\alpha\beta}B^{\alpha\beta} \quad , \quad \mathcal{O}_{T,9} = B_{\alpha\mu}B^{\mu\beta}B_{\beta\nu}B^{\nu\alpha} \, .$$

M (mixed) operators

affect mixed polarization

$$\mathcal{O}_{M,0} = \mathrm{Tr}\left[\widehat{W}_{\mu\nu}\widehat{W}^{\mu\nu}\right] \times \left[(D_\beta\Phi)^\dagger D^\beta\Phi\right] \quad , \quad \mathcal{O}_{M,1} = \mathrm{Tr}\left[\widehat{W}_{\mu\nu}\widehat{W}^{\nu\beta}\right] \times \left[(D_\beta\Phi)^\dagger D^\mu\Phi\right]$$
$$\mathcal{O}_{M,2} = \left[B_{\mu\nu}B^{\mu\nu}\right] \times \left[(D_\beta\Phi)^\dagger D^\beta\Phi\right] \quad , \quad \mathcal{O}_{M,3} = \left[B_{\mu\nu}B^{\nu\beta}\right] \times \left[(D_\beta\Phi)^\dagger D^\mu\Phi\right]$$
$$\mathcal{O}_{M,4} = \left[(D_\mu\Phi)^\dagger \widehat{W}_{\beta\nu}D^\mu\Phi\right] \times B^{\beta\nu} \quad , \quad \mathcal{O}_{M,5} = \left[(D_\mu\Phi)^\dagger \widehat{W}_{\beta\nu}D^\nu\Phi\right] \times B^{\beta\mu} + \mathrm{h.c.}$$
$$\mathcal{O}_{M,7} = \left[(D_\mu\Phi)^\dagger \widehat{W}_{\beta\nu}\widehat{W}^{\beta\mu}D^\nu\Phi\right] \, .$$

↗ Eboli et.al.

nTGC Dim-8 EFT Operators

Trilinear coupling between Z and photons

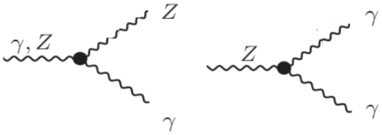

$$\begin{aligned}
\mathcal{O}_{BW} &= i\, H^\dagger B_{\mu\nu} W^{\mu\rho} \{D_\rho, D^\nu\}\, H, \\
\mathcal{O}_{WW} &= i\, H^\dagger W_{\mu\nu} W^{\mu\rho} \{D_\rho, D^\nu\}\, H, \\
\mathcal{O}_{BB} &= i\, H^\dagger B_{\mu\nu} B^{\mu\rho} \{D_\rho, D^\nu\}\, H. \\
\mathcal{O}_{\widetilde{B}W} &= i\, H^\dagger \widetilde{B}_{\mu\nu} W^{\mu\rho} \{D_\rho, D^\nu\}\, H,
\end{aligned}$$

Saskia Falke - Ecole de Gif 2023

Fermionic Dim-6 Operators: Examples (Warsaw Basis)

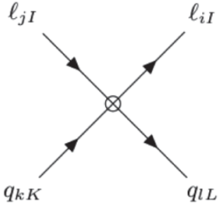

$$i(C_{\ell q}^{(1)ijlk}\delta_{IJ}\delta_{KL}+ \\ +C_{\ell q}^{(3)ijlk}\tau^a_{IJ}\tau^a_{LK})\gamma^\alpha P_L\otimes\gamma_\alpha P_L$$

PhysRevD.105.096040

$c_{Hl}^{(3)}$	$(H^\dagger i \overleftrightarrow{D}^I_\mu H)(\bar{l}_p\tau^I\gamma^\mu l_r)$	
$c_{Hq}^{(3)}$	$(H^\dagger i \overleftrightarrow{D}^I_\mu H)(\bar{q}_p\tau^I\gamma^\mu q_r)$	

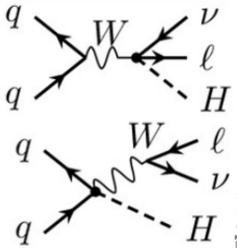

S. Falke

ATLAS Diboson

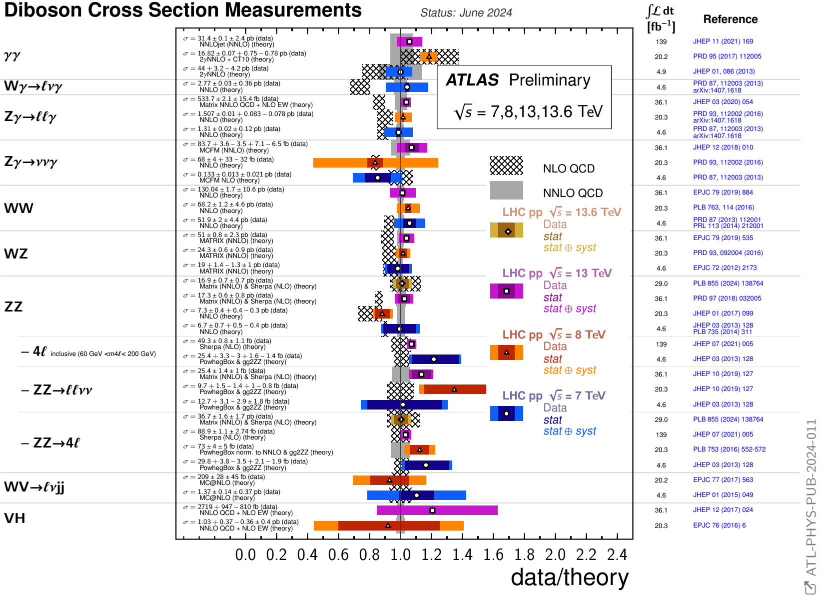

ATLAS Triboson & VBS

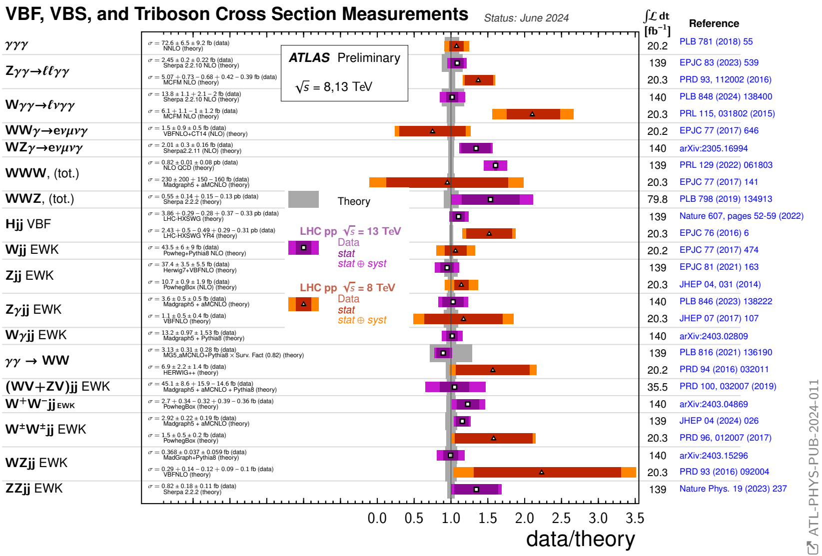

CMS Diboson & Triboson & VBS

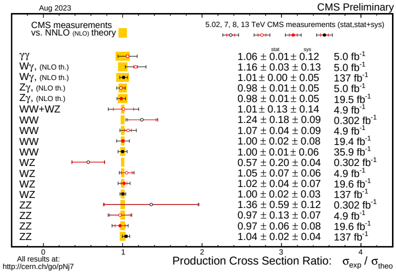

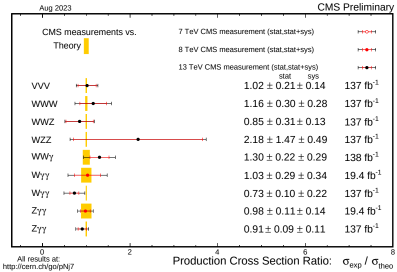

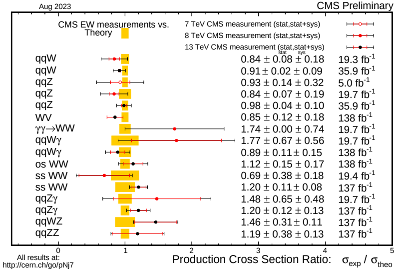

CMS-SM-Summary-Plots